Structural Safety 48 (2014) 15–24

Contents lists available at ScienceDirect

Structural Safety

journal homepage: www.elsevier.com/locate/strusafe

Multi-dimensional hurricane resilience assessment of electric power systems

Min Ouyang [a,*], Leonardo Dueñas-Osorio [b]

[a] School of Automation, Huazhong University of Science and Technology, 1037 Luoyu Road, Wuhan 430074, China
[b] Department of Civil and Environmental Engineering, Rice University, 6100 Main Street, MS-318, TX 77005, United States

ARTICLE INFO

Article history:
Received 9 October 2012
Received in revised form 14 January 2014
Accepted 26 January 2014

Keywords:
Electric power systems
Resilience
Hurricane hazards
Component fragility
Robustness
Restoration
Networks

ABSTRACT

Electric power systems are critical to economic prosperity, national security, public health and safety. However, in hurricane-prone areas, a severe storm may simultaneously cause extensive component failures in a power system and lead to cascading failures within it and across other power-dependent utility systems. Hence, the hurricane resilience of power systems is crucial to ensure their rapid recovery and support the needs of the population in disaster areas. This paper introduces a probabilistic modeling approach for quantifying the hurricane resilience of contemporary electric power systems. This approach includes a hurricane hazard model, component fragility models, a power system performance model, and a system restoration model. These coupled four models enable quantifying hurricane resilience and estimating economic losses. Taking as an example the power system in Harris County, Texas, USA, along with real outage and restoration data after Hurricane Ike in 2008, the proposed resilience assessment model is calibrated and verified. In addition, several dimensions of resilience as well as the effectiveness of alternative strategies for resilience improvement are simulated and analyzed. Results show that among technical, organizational and social dimensions of resilience, the organizational resilience is the highest with a value of 99.964% (3.445 in a proposed logarithmic scale) while the social resilience is the lowest with a value of 99.760% (2.620 in the logarithmic scale). Although these values seem high in absolute terms due to the reliability of engineered systems, the consequences of departing from ideal resilience are still high as economic losses can add up to $83 million per year.

1. Introduction

Modern society and its economy depends on critical infrastructure services, such as electricity, water, gas and oil, and telecommunication networks. However, infrastructure systems are confronted with numerous problems, such as unavoidability of damage due to natural hazards (e.g., earthquakes, hurricanes, floods), component aging, demand increase, and climatic change, all of which increase their failure probabilities and risks. Hence, the assessment of performance and recovery of these systems is required to support their rapid restoration as well as the needs of the population in their service areas. Modeling the resilience of these systems is necessary to understand their risks and to support infrastructure system design or improvement decisions [1]. Among infrastructure systems, electric power systems are particularly critical, because most other lifeline systems need electricity for their operation and management. This paper takes a power system located near the Gulf Coast of the United States where hurricane hazards are frequent (on average once in 7 years [2]), as a practical example to illustrate a proposed resilience assessment approach.

Regarding the term "resilience", engineering scholars and institutes have proposed different definitions [3–6]. Broader resilience definitions in various fields are summarized by Plodinec [7]. Considering the available literature, from an infrastructure engineering, the authors recently defined resilience as the joint ability of distributed systems, such as electric power systems, to *resist* (prevent and withstand) multiple possible hazards, *absorb* the initial damage, and *recover* to normal operation [8]. To quantify the resilience of engineered systems, the Multidisciplinary Center for Earthquake Engineering Research (MCEER) introduced a general framework to measure seismic resilience [9], which can also be applied in infrastructure systems under other hazard types and is then adapted in this paper to the context of power systems in hurricane-prone areas. Resilience in the MCEER framework includes four properties: robustness, redundancy, resourcefulness, and rapidity, where resilience itself is quantified via four

* Corresponding author. Tel.: +86 18071749645.
E-mail addresses: min.ouyang@hust.edu.cn (M. Ouyang), leonardo.duenas-osorio@rice.edu (L. Dueñas-Osorio).

http://dx.doi.org/10.1016/j.strusafe.2014.01.001
0167-4730/

interrelated dimensions: technical, organizational, social and economic. In addition, the four properties of each dimension of resilience can be quantified by different performance measures. Taking the robustness property as an example, the technical, organizational, social, and economic dimension performance measures might respectively be the availability of operational power supply, availability of emergency organizations and critical functions, the percentage of households with power, and the percentage of all businesses with power immediately after a disruptive event. Under this MCEER framework, several studies have emerged on the application of resilience quantification to hospitals [10,11], communities [9,12], and some networked utility systems [13,14]. Defined resilience metrics in the literature typically include the area between the target performance curve and the real performance curve within the restoration period [9,10,15], the probability of meeting predefined system-level performance standards in a scenario event [12], a normalized area underneath the system performance curve in a single event [11,13] (see typical system performance curve in Section 2), a normalized and weighted sum of the disaster consequences and the recovery effort [14], or a function of the system performance drop immediately after an event along with the required restoration time [16].

As the above studies are usually aimed at resilience assessment for specific events, the authors then introduced a resilience framework for infrastructure systems, which is not only adequate for single and multiple hazards [8], but also adequate for quantifying potential future resilience with the consideration of system evolution [17]. In such a framework, an artificial betweenness-based flow model and a simple restoration model were used to assess hurricane resilience of a power system for illustrative purposes. However, this flow model departs from electrical flow models of the power system for response or vulnerability analyses under disruptive events [48]. Hence, after detailed studies of the emergency operation plans of utility companies for hurricane events and collecting the power outage and restoration data after some hurricane events, this paper proposes a new more elaborate yet practical probabilistic model for the hurricane resilience assessment of power systems, where the power flows are captured by a DC-based model, and the event consequences are measured from multiple dimensions while the whole resilience model is calibrated according to historical failure data.

The proposed resilience model includes four types of interrelated sub-models, including a hazard scenario generation model, component fragility models, a power system performance model, and a system restoration model. Some sub-models have been integrated together in the literature for different system-level performance studies, not necessarily resilience-based, under different hazards. For example, scholars used the first three types of sub-models together to investigate power grid vulnerability under different hazard types, such as the hurricane vulnerability of several power grids in Texas [29], seismic vulnerability of power grids as well as their interdependent gas or water systems in Europe [18] and Shelby County, USA [19,20], the terrorism vulnerability of power grid as well as its interdependent water supply, steam supply and natural gas systems at the Massachusetts Institute of Technology (MIT) campus [21], and the lightning vulnerability of the IEEE 118-node power grid [22]. Other scholars have integrated the four types of sub-models together to analyze infrastructure restoration, such as the post-earthquake restoration planning and optimization of Los Angeles power and water systems [23,24], the weather-induced power grid response and restoration [25], and the seismic resilience assessment and improvement of Memphis water systems [12]. Based on these previous works and the resilience definition and quantification equations proposed by the authors [8], this paper adapts and applies the four types of sub-models to a relevant gap problem, namely that of electric power systems under hurricane hazards to assess their multi-dimensional resilience, where the power system is modeled as an open flow-based system to better approach practical constraints, while the restoration process is modeled based on historical hurricane restoration practices.

The rest of this paper is organized as follows: Section 2 introduces a probabilistic model for hurricane resilience assessment. Based on outage and restoration data from Hurricane Ike in 2008 for the power system in Harris County, Texas, USA, Section 3 describes the model calibration. Then hurricane resilience is assessed and analyzed in Section 4. Finally, Section 5 provides conclusions and future research directions.

2. Probabilistic resilience assessment model

In previous work [8], the authors introduced a time-dependent expected resilience metric for networked systems that builds upon the system performance and response process following a disruptive event as shown in Fig. 1. The process can be divided into three different stages: the disaster prevention stage ($0 \leqslant t \leqslant t_0$), the damage propagation stage ($t_0 < t \leqslant t_1$), and the assessment and recovery stage ($t_1 < t \leqslant t_E$). These three stages constitute a typical response cycle, and can respectively reflect resistant, absorptive and restorative capacities of a system. During a time period from 0 to T, there may exist many response cycles. The three capacities reflected within T together determine infrastructure resilience over that time horizon.

In the figure, there are two time-dependent curves. The first is the target performance curve $P_T(t)$, which is typically modeled as constant but could vary with time. The second is the real performance curve $P_R(t)$, recording change under major disruptive events and system restoration efforts. Resilience can then be quantified in general as the ratio of the areas between the curve $P_T(t)$ and the time axis and the curve $P_R(t)$ and the time axis within the time period from 0 to T:

$$R(T) = \int_0^T P_R(t)dt \Big/ \int_0^T P_T(t)dt \tag{1}$$

Note that this resilience metric is different from those measures proposed in previous studies [9–11,13,15], which have similar forms with Eq. (1) but their integration time interval is $[t_0, t_E]$. Hence, those metrics in previous studies quantify resilience for specific disruptive events and not sequences of them, and could not totally account for the resistant ability of resilience (to prevent and withstand multiple types of events). Note that the value of $R(T)$ is bounded in the range [0, 1]. Hence, if the curves $P_R(t)$ and $P_T(t)$ are measured by the same metrics, but with different aims such

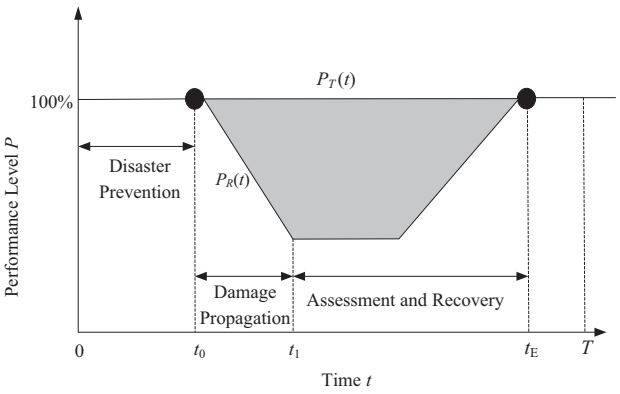

Fig. 1. Typical performance curve of an infrastructure system following a disruptive event (adapted from reference [8]).

as the amount of flow or services delivered, the availability of critical facilities, the number of customer served, or the support of economic activities, then Eq. (1) corresponds to the technical, organizational, social, and economic dimensions of resilience, respectively, and can be used for comparative studies.

Different periods relative to when T is achieved yield different forms of resilience [17]: (1) *previous resilience* estimated based on historical data within a time period $[0, T]$ that has already occurred, (2) *current potential resilience* with the system parameters (such as power supply, power demand, network topology, line parameters, etc.) fixed during the time range up to T and equal to current time settings, and (3) *future potential resilience*, which is similar to (2) but with the additional consideration of system improvement and evolution processes (supply/demand change, topological evolution, etc.). This paper mainly investigates the current potential resilience and focuses on the introduction of multi-dimensional (technical, organizational, and social) resilience assessment, along with an estimation of the economic losses as an alternative to full economic resilience assessment, which ideally needs to consider the loss of gross regional product (GRP) [9]. The future potential resilience is studied for power system under random failures in Ouyang and Dueñas-Osorio [17].

For the case in which the current potential resilience, $P_T(t)$ is assumed to be a constant value equal to 1.0. When a hazard of interest has its occurrence governed by a Poisson process, such as the hurricane hazards in this paper, the expected resilience $E[R(T)]$ of Eq. (1) is [8]:

$$\begin{aligned} E[R(T)] &= E\left[\frac{\int_0^T P_R(t)dt}{T}\right] = E\left[\frac{T-\sum_{n=1}^{N(T)} IA_n(t_n)}{T}\right] \\ &= 1 - E\left[\frac{1}{T}\sum_{n=1}^{N(T)} IA_n(t_n)\right] = 1 - \frac{1}{T}\sum_{N=0}^{\infty} N \times E[IA]\frac{(\lambda T)^N e^{-\lambda T}}{N!} \\ &= 1 - \lambda E[IA] \end{aligned} \tag{2}$$

where $E[\bullet]$ is the expected value; n is the event occurrence number; $N(T)$ is the total number of event occurrences during T; t_n is the occurrence time of the nth event, which is a random variable; $IA_n(t_n)$ is the area between the real performance curve and the targeted performance curve, called impact area for the nth event occurrence at time t_n; $E(IA)$ is the expected impact area under the hazard accounting for all possible hazard intensities; and λ is the occurrence rate of the hazards per year. Eq. (2) indicates that the current potential resilience has an expected value not directly related with the time period T.

2.1. Description of electric power systems

The electric power system in Harris County, Texas, United States is a main part of the power system owned and maintained by CenterPoint Energy, which delivers electricity to over 2.26 million customers in a 12,950 km^2 service area around greater Houston. The studied system approximately serves 1.7 million customers, and includes high voltage (35–345 kV) transmission networks and low voltage (0.12–35 kV) distribution networks.

The transmission network in Harris County is obtained from Platts [26]; its geographical representation is shown in Fig. 2(a). This system has 23 power plants and 394 substations connected by 551 transmission lines. The power plant capacities are obtained from the Platts' database, and the technical parameters for lines, such as reactance and capacity, are estimated according to conductors' properties [27]. It is an open system, and connects with other systems outside the studied area via transmission lines. Most of the substations connecting with the outside area link with some power plants via less than 2 substations. Hence, this paper models these substations as virtual power plants, each with the capacity equal to the sum of the capacities of their attached outgoing transmission lines.

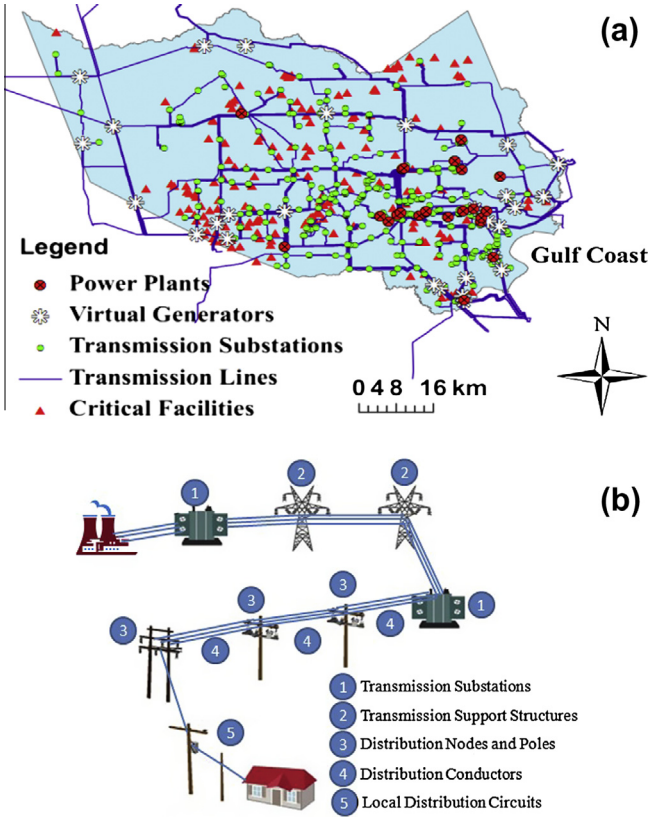

Fig. 2. (a) A geographical representation of the power transmission network in Harris County, Texas, along with the sites of critical facilities; (b) a schematic figure to illustrate some power system components whose hurricane fragilities are mainly considered in the paper (The component icons are extracted from reference [53]).

Regarding the electric distribution network, it is not available for analysis due to security concerns. However, the "distribution circuits are found along most secondary roads and streets" [28]; hence, similar to the work by Winkler et al. [29], this paper uses an idealized distribution network synthesized from the local road network information. Each intersection of the road network is extracted as a proxy distribution node, which is connected to the nearest transmission substation. The loads of these distributed nodes in the same census tract are estimated proportionally to the number of households in that tract. With these assumptions, each distribution node serves an average of 40 customers [30]. The electricity from a distribution node to its served customers is supplied via local distribution circuits. Also, the geographical sites of critical facilities, such as hospitals, gas compressors, and water pump stations, are shown in Fig. 2(a) for the resilience analysis that follows. Fig. 2(b) shows a schematic plot of some of the above components and their relationships. The labeled components and their fragilities are used in this study for hurricane resilience assessment.

2.2. Hurricane hazard model

Hurricane events are described by a Poisson process of constant rate λ_h such that the time between each pair of consecutive hurricane events has an exponential distribution with a probability function as shown in Eq. (3) [30].

$$f(t) = \begin{cases} \lambda_h e^{-\lambda_h t} & t \geqslant 0 \\ 0 & t < 0 \end{cases} \tag{3}$$

According to historical data from 1900 to 1999 [31], the return periods of hurricanes with maximum category x or higher (x = 1, 2, 3, 4, 5) when they pass the Harris County area are respectively 7, 15, 25, 53, and 140 years. Hence, the annual occurrence rate of hurricane hazards with category 1 or higher is λ_h = 1/7/year, and the probability of a hurricane belonging to each category given it occurs is respectively 0.53, 0.19, 0.15, 0.08, and 0.05. To obtain the wind gusts at the different sites of infrastructure components under a hurricane event, the HAZUS-MH3 software [32] is used to generate hurricane scenarios by activating probabilistic hurricane hazards (which can produce many hurricane scenarios with different return periods) or manually defining different hurricane tracks (a hurricane track consists of several points along the track, and each of the points is specified by some storm parameters, such as latitude, longitude, elapsed time, radius to maximum winds, maximum wind speed, central pressure and so on). A generated hurricane scenario is grouped to a category according to its maximum category over the whole county; then, 50 different scenarios for each hurricane category are generated. Fig. 3 shows a generated hurricane scenario grouped into category 3 by manually defining a hurricane track. The maximum sustained wind speeds at different sites vary from 73 to 137 mph. Note that the design wind speeds in Harris County according to ASCE 7-05 criteria range from 90 to 120 mph, depending on the distance to the coast. A hurricane with category 3 or higher can cause extensive damage in the county.

To simulate hurricane hazards during a time period from 0 to T, an occurrence time is first determined by adding a random value generated based on Eq. (3) to the last hurricane occurrence time or zero (if no hurricane has occurred before). If the occurrence time is less than T, select a hurricane category according to the above hurricane category probabilities 0.53, 0.19, 0.15, 0.08, and 0.05, and then select a pre-generated HAZUS hurricane scenario at random from the scenarios already grouped per category. The specific wind gust speeds at different sites are then used for the subsequent component fragility analysis. Moving to the next hurricane occurrence time until the time T provides a realization of hurricane hazards during [0, T]. Note that this hurricane event generation process enables the occurrence of more than one hurricane within 1 year.

2.3. Component fragility model

Although power systems include many types of components, it is practical to mainly focus on the response of the most critical and vulnerable ones. Hence, this paper considers the following five component types: transmission substations, transmission lines (including transmission support structures and the conductors between structures), distribution nodes, distribution lines (including distribution poles and the conductors between poles), and local distribution circuits, which deliver electricity from each distribution node to its served customers. Some other hurricane-related reports from other regions, such as electric utilities in Florida by Quanta Technology [30], also considered components like the five selected here. A schematic plot of these components and their relationships is displayed in Fig. 2(b). Since power plants are mostly impervious to structural hurricane damage (with the exception of hurricane-induced flooding), their fragility is not considered here.

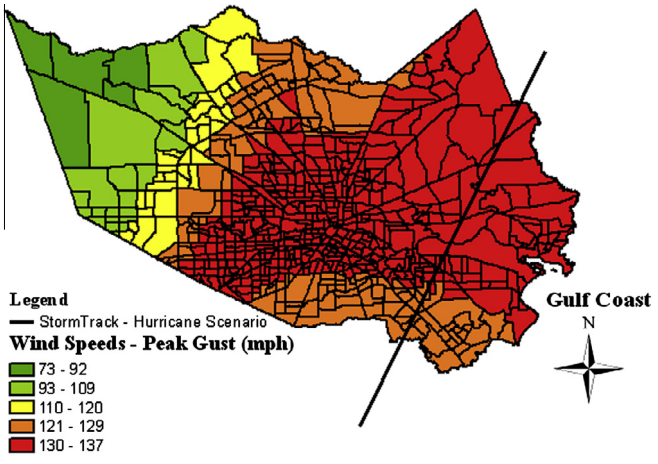

Fig. 3. A hurricane scenario in Harris County grouped into category 3 generated by manually defining a track.

Regarding the failure probability $p_{f,trans\_sub,i,j}$ of the ith transmission substation, it is represented by a lognormal fragility curve,

$$p_{f,trans\_sub,i,j}(D \geqslant d_{i,j} | W_s = x_i) = \int_0^{x_i} \frac{1}{\sqrt{2\pi}\sigma_{i,j} w} \exp\left(\frac{-(\ln w - \mu_{i,j})^2}{2\sigma_{i,j}^2}\right) dw \quad (4)$$

These curves generate four probabilities, $p_{f,trans\_sub,i,low} > p_{f,trans\_sub,i,low} > p_{f,trans\_sub,i,moderate} > p_{f,trans\_sub,i,complete}$, for the substation damage D exceeding a certain level $d_{i,j}$ with j = {low, moderate, severe, complete} for a given wind gust speed $W_s = x_i$ (m/s) while taking into account the local terrain and structural characteristics of the substation under consideration. The values of $\mu_{i,j}$ and $\sigma_{i,j}$ of the fragility curves for each damage level $d_{i,j}$, and each type of modeled terrain and building type are taken from HAZUS-MH3 [32]. By comparing the four probabilities with a uniformly distributed random variable within [0, 1] one can determine the damage level realizations per substation. Then, based on HAZUS-MH3 data [32], for each failed substation, a repair time in hours (h) could be assigned, which satisfies a normal distribution $t_{r,trans\_sub,i,j} \sim N(24h, 12h)$, $N(72h, 36h)$, $N(168h, 84h)$, $N(720h, 360h)$, while the repair costs are respectively \$0.3 million, \$1.1 million, \$5.5 million and \$10.0 million. In addition, if a substation acting as a virtual power plant does not fail, its virtual capacity is set based on the states of their attached incoming transmission lines which connect it with real power plants outside the studied area.

Transmission lines consist of transmission support structures (e.g., towers and poles), conductors and various pieces of hardware. Due to design requirements [33], the fragility of a transmission line under wind loads (barring debris potential which could be incorporated as a Poisson process in future work) is mainly determined by the failures of support structures. The number of transmission supports along a line is computed as the line length divided by the average span between two adjacent towers or poles, which is set as 0.23 km based on regional utility data [34]. For each support structure, different utilities may use different fragility curves as the best fit according to historical data. Based on the investigations by Quanta Technology [34], the failure probability $p_{f,support\_struct,i}$ of the ith transmission support structure in the studied area can be approximated by an exponential function under a given wind speed $W_s = x_i$,

$$p_{f,support\_struct,i}(W_s = x_i) = \min\{2 \times 10^{-7} e^{0.0834 x_i}, 1\} \quad (5)$$

The restoration time for a transmission support structure failure i is also assumed to satisfy the normal distribution $t_{r,support\_struct,i} \sim N(72h, 36h)$, with a repair cost of \$0.4 million [35].

In terms of distribution nodes, these are modeled as distribution poles. Similar to the transmission support structures, the failure rate of the ith distribution pole is modeled by an exponential function [34],

$$p_{f,dist\_pole,i}(w_s = x_i) = \min\{0.0001e^{0.0421x_i}, 1\} \quad (6)$$

The restoration time for a failed distribution pole i is also assumed to satisfy the normal distribution $t_{r,dist\_pole,i} \sim N(5h, 2.5h)$, with a repair cost of \$2500.0 [30].

The distribution line from a substation to a distribution node consists of distribution poles which are different from the distribution nodes that directly connect with the customers; the poles here are just a part of the distribution lines; they also consist of conductors (a small segment of the distribution line between poles), and other equipment types. Poles and conductors are mainly considered for the fragility estimation of entire distribution lines l, which are modeled as series systems with each pole or conductor fragility estimated by Eq. (6) or (7). The average span between two distribution poles is set as 0.042 km based on utility data [34]. The conductors between two distribution poles, different from the transmission conductors, are much more prone to failures due to distinct factors such as falling trees and flying debris. Based on Winkler et al.'s work [29], the failure probability of the kth distribution conductor between two poles is modeled by:

$$p_{f,conductor,k} = (1 - f_u)\max(p_{f,wind,k},\ \alpha p_{f,windthrow,k}) \quad (7)$$

where $p_{f,wind,k}$ is the direct wind-induced damage probability of conductor k; $p_{f,windthrow,k}$ is the probability of tree wind-throw (trees uprooted or broken by wind) near the conductor k; f_u is the probability of conductor k being underground (invulnerable to hurricane events) – set as 0.32 according to utility data [34]; and α is the average tree-induced damage probability of overhead conductors in the case of tree wind-throw near the conductor, which can reflect the efforts of trimming trees by power companies and is assumed constant as a first approximation. The parameter $p_{f,wind,k}$ is simply computed by

$$p_{f,wind,k} = \min\{F_{wind,k}/F_{force,k}, 1\} \quad (8)$$

where $F_{wind,k}$ is the wind loading on the conductor and can be calculated according to practical design recommendations [36], $F_{force,k}$ is the maximum perpendicular force that the line can endure and can be estimated according to the conductor property parameters [27]. Note that strictly speaking, the $p_{f,wind,k}$ should be a more complicated increasing function of the ratio $F_{wind,k}/F_{force,k}$, but due to lack of sufficient data to fit the function, this paper simply models $p_{f,wind,k}$ by Eq. (8) as an initial approximation. The probability of wind-throw $p_{f,windthrow,k}$ can be computed by [37]:

$$\log(p_{f,windthrow,k}/(1 - p_{f,windthrow,k})) = a_s + c_s(k_z S_k)D_H^{b_s} \quad (9)$$

where a_s, b_s, and c_s are species specific constants, S_k the wind intensity (0–1 scale) at the conductor, and D_H the tree diameter at breast height. The S_k parameter is generated by dividing the local wind hazard by the maximum wind hazard in the studied region. The factor k_z adjusts the hazard intensity to account for local terrain effects, and is chosen based upon the land cover information near the conductor [36]. Tree coverage in Harris County is captured by terrain types, such as developed (high), deciduous forest, evergreen forest, shrubs, crops and other 24 types [38]. Note that if the tree coverage data immediate adjacent to power lines are available, it is better to use them instead of the tree coverage data in the census tract including the power lines to model the tree wind throw. Also, the restoration time of a failed conductor k has the distribution $t_{r,conductor,k} \sim N(4h, 2h)$, with a repair cost of \$1500.0 [30].

Finally, local distribution circuits supply electricity from a distribution node to its customers. The fragilities of such local circuits are simply modeled by the percentage of outage customers $p_{f,customer,i}$ associated with a distribution node i,

$$p_{f,customer,i} = \beta(1 - f_u)p_{f,windthrow,i} \quad (10)$$

where $p_{f,windthrow,i}$ is the probability of tree wind-throw near distribution node i, $1 - f_u$ is the percentage of overhead lines, and β is the average probability that customers will be out of power due to damage on local distribution circuits in the case of tree wind-throw, which can also reflect the efforts of trimming trees locally by power companies and is assumed constant as well. The restoration time for each outage customer has the distribution $t_{r,customer,j} \sim N(0.5h, 0.25h)$. The damage cost on local distribution circuits is ignored here due to the unknown exact configurations of local distribution circuits. However, such costs can be indirectly reflected in the customer interruption cost, which is \$2.99 per customer per outage hour [39].

2.4. Power system response model

Many models have been proposed to capture power system responses after component failures, such as the DC-based OPA models (a joint effort from the U.S. Oak Ridge National Laboratory, the Power System Engineering Research Center at the University of Wisconsin-Madison, and the University of Alaska) [40], AC-based power flow models [41], hidden failure models [42], complex network based models [22], and stochastic models [25]. Based on these existing models and with the objective of including restoration practices, this paper models the power system response as follows:

Component failures first alter the power grid topology, and may separate the power grid into many unconnected sub-grids. For each sub-grid, the system response is modeled according to the following rules: (1) If it does not contain any power plant, then all the load nodes in this sub-grid are assumed failed (in terms of service); (2) If the sum of all power plant capacities inside the sub-grid is larger than the sum of the demand, then cut the output of power plants uniformly to balance the total supply and total demand, and then check the line flow constraints after running a DC power flow model; if there are violations, cut the load to the smallest number of customers until the line constraints are satisfied; (3) If the sum of all power plant capacities inside the sub-grid is smaller than the sum of the demand, cut the load to the smallest number of customers first to balance the total supply and total demand, and then follow the same procedures in step (2). The DC power flow equations provide a linear relationship between the power flow vector $\boldsymbol{F}$ (consisting of the flow through each line) and the power injection vector $\boldsymbol{P}$ at the nodes (if a node is a power plant, its power injection is a positive electricity quantity; if a node is a load node, its power injection is a negative load level; and if a node is a transshipment node, its power injection is zero). It can be written as:

$$\boldsymbol{F} = \boldsymbol{A}\boldsymbol{P} \quad (11)$$

where $\boldsymbol{A}$ is a constant matrix, whose elements can be calculated in terms of the reactance of the lines [40]. When the balance between total supply (sum of outputs from power plants) and total demand (sum of consumption from customers or loads) and the line flow constraints (lines' flow less than their capacities) are satisfied, the system reaches the steady state and then performance metrics can be computed.

2.5. Restoration model

There is emerging literature studying the restoration process of power systems under hurricane events [43–45]. However, these studies use statistical methods to predict the restoration times and could not consider the effects of different restoration sequences to support resilience assessment, which requires modeling of restoration processes under different damage states of the system and its many critical components. By studying the emergency response plan as well as the reports from CenterPoint Energy

after Hurricane Ike [46], this paper models a generic restoration process by capturing two critical factors, which enable expanding over traditional reliability analyses, while including simplifications to allow for initial resilience studies.

The first factor is the mobilization of restoration resources. There are different types of resources for different types of restoration activities. To model resource quantities, this paper considers all resources with the same effectiveness, and one unit of restoration resources refers to a repair team, including repair crews, vehicles, equipment and some replacement components. Each damaged component needs one unit of restoration resources for recovery, and the restoration times for different damages are set according to the probability distributions introduced in Section 2.3. Also, CenterPoint Energy and most utilities are part of electric utility mutual assistance programs to access linemen and tree trimmers from around the country. Hence, after hurricane events, the local amount of restoration resources could increase with time. An increasing function is thus used to characterize the dynamic process of resource mobilization.

The second factor is the restoration sequence. According to documents and reports from the local utility company, this paper models the restoration priority according to the following rules: First, repair transmission substations, transmission lines, and critical facilities vital to public safety, health and welfare, such as hospitals, water treatment plants and public service facilities. This paper considers three types of critical facilities in the studied area: hospitals, gas compressors, and water pumping stations, with their combined geographical sites shown in Fig. 2(a). These critical facilities are assumed to get long-term electricity from their nearest distribution nodes. For each of all these damaged components within the first-step repair group, compute the minimum repair time (*MRT*) required to access any one of the power plants; the smaller the *MRT* is, the higher repair priority it has.

Second, repair the distribution lines from substations to distribution nodes that can restore power to the greatest number of customers in the least amount of time. However, in practice, the above rules may not be strictly obeyed due to difficult access to the damaged components or some economic concerns [47]. To capture this feature, among all the remaining damaged distribution lines, a distribution line l is selected to be repaired with the following probability:

$$p_{repair,l} = (C_l/t_{dist\_line,l})^{\gamma} / \sum_{l \in L_D} (C_l/t_{dist\_line,l})^{\gamma} \tag{12}$$

where C_l is the number of served customers by distribution line l, $t_{dist\_line,l}$ is the required restoration time for line l, estimated as the maximum value of repair times $t_{r,dist\_pole,i}$ and $t_{r,conductor,j}$ of all damaged distribution poles (i) and distribution conductors (j) along the line l; L_D is the set for all remaining damage distribution lines, while γ is a sequence control factor. For $\gamma \in (-\infty, +\infty)$, $p_{repair,l} \in [0, 1]$. Note that the variables C_l, $t_{dist\_line,l}$ and L_D in Eq. (12) are modeled as deterministic because restoration decisions are made after the utility companies know, even if imperfectly, the damage states of their power grid components and their repair times, while γ is a tunable variable, depending on the access to the damaged components or economic availability concerns during the restoration process. Specifically, if $\gamma = 0$, $p_{repair,l} = 1/|L_D|$ (where $|L_D|$ is the number of remaining damage distribution lines), each damaged line k has the same associated value of $p_{repair,l}$, and is then randomly selected for repair; if $\gamma \to +\infty$, $p_{repair,l} \to 1$, the damaged line l with the largest ratio of C_l to $t_{dist\_line,l}$ is selected to repair first, and the above restoration sequences are thus strictly followed. For each of the damaged components along the distribution line l, the closer the position it is to the substation, the higher repair priority it has.

Third, repair the local distribution circuits delivering power from distribution nodes to their served individual customers. The larger number of customers a local distribution circuit serves, the higher repair priority it has.

When the above four models from Sections 2.2–2.5 work together, a restoration curve can be simulated to quantify the real performance curve $P_R(t)$ under a hurricane scenario (Fig. 1), which supports the resilience estimation based on Eq. (1). In fact, the resilience quantification here can go beyond a single hazard scenario. In addition, based on the performance curves, the economic loss consisting of the repair cost of damaged components and the customer power interruption cost can be estimated to enrich the multi-dimensional resilience perspectives.

3. Resilience model calibration

Hurricane Ike made landfall in Galveston, Texas, on September 13, 2008. At landfall, it was a large category 2 hurricane with hurricane force winds extending 443 km from the center. The event caused extensive failures to the electric power system in Harris County, which happened to be relatively well documented. This paper uses available data of the number of customers without power and their restoration after Hurricane Ike for model calibration. Harris County land cover data is obtained from the Multi-Resolution Land Characteristics Consortium to support the estimation of component fragilities, while the specific Hurricane Ike scenario for Harris County is provided by HAZUS-MH3 [32]. Given the wind speed at each component site, failures are evaluated according to component fragility models by using Monte Carlo simulation, and then the DC power flow model is used to simulate the functional state of each physical component to then calculate the percentage of customers without power, which are further aggregated to the postal (ZIP) code level to compare with the percentage of customers without power per ZIP code reported by CenterPoint Energy immediately following Hurricane Ike [46]. Running the simulation 500 times until the average percentage of customers without power in each ZIP converges to a deviation of less than 0.001, the absolute error for the zth ZIP code can be calculated as the absolute difference of the percentage of customers without power in the simulation and in the actual record for that ZIP code. The mean error of this absolute error over all ZIP codes is taken as the objective function to calibrate the parameters α and β, where α is average tree-induced damage probability of overhead conductor in the case of tree wind-throw near conductors, and β is average probability that customers will be out of power due to damage on local distribution circuits in the case of tree wind-throw. These two parameters are related to trees and have influence in local-level component damage. The minimum mean error over all ZIP codes is found to be 14.15%, with the corresponding parameters being $\alpha = 0.35$, $\beta = 0.54$. The value of β matches well with the data (0.53) from a survey conducted by the authors' hurricane research group [49].

Next, based on the above parameter settings, and taking the repair resource mobilization curve into consideration, it is possible to simulate the system restoration curve, i.e., the relationship between the percentage of customers with power and time after landfall. For the resource mobilization curve, according to the post-Hurricane-Ike reports from CenterPoint Energy [46], it can be approximately captured by the curve shown in Fig. 4. The parameter $RR1$ indicates the number of repair resources owned by the company itself, while the subsequent increase to $RR2$ is due to the assistance from other utility companies. According to real data, set $RR1 = 720$ repair teams, and $RR2 = 1{,}995$ repair teams, corresponding to a resource increase of $I_R = 15$ repair teams per hour from time 25 to 109. Under various restoration sequence

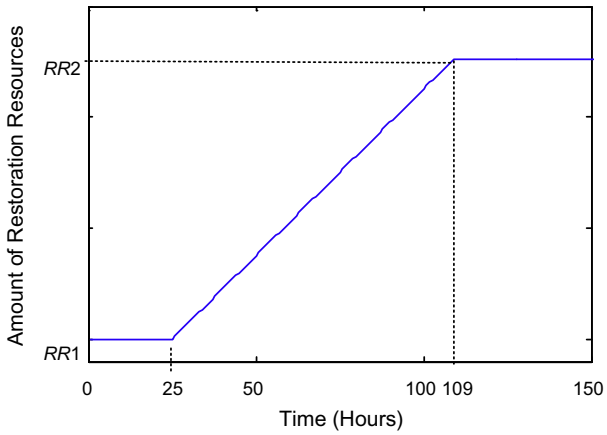

Fig. 4. Approximate shape of the relation between the amount of restoration resource units and time immediately after Hurricane Ike in 2008.

control factors γ, different restoration sequences are simulated, and it is found that $\gamma = 0.8$ makes the simulated restoration curve consistent with the actual curve from Hurricane Ike, as shown in Fig. 5. The minimum/maximum error bars are also presented in the figure, and the small error bars indicate small fluctuation and uncertainty to input variability of the proposed model. Also, the cases of $\gamma = 0$ (random restoration sequences) and $\gamma \to \infty$ (restoration rules strictly obeyed sequences) are presented in the figure for comparisons.

From the figure, when $\gamma = 0$, after assigning the restoration resources to transmission substations, transmission lines and critical facilities, the damaged distribution lines are then randomly selected for repair, which leads to an approximately uniform increase of the percentage of restored customers. Hence, the curve at $\gamma = 0$ is almost linear. When $\gamma \to \infty$, the damaged distribution lines are repaired strictly based on the rules which first repair the line with the largest ratio of C_l to $t_{dist\_line,l}$. Hence, the restoration speed is high early on, and then it increases at a decreasing rate until around time 330, when most curves converge, as shown in Fig. 5. After time 330, all distribution lines have been restored, and all crews start to repair the local distribution circuits to restore power to remaining individual customers. As the restoration time for each outage customer has an identical distribution, the restoration speed after time 330 is almost constant and the curves are all linear at different γ.

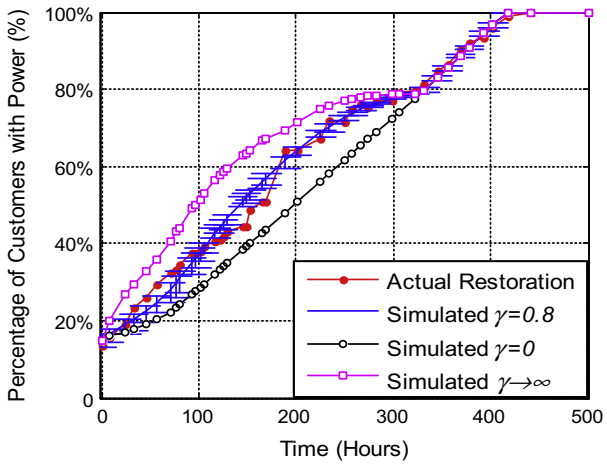

Fig. 5. Comparisons between the actual restoration curve and the simulated curves. The minimum/maximum error bars from 500 simulations are also presented. Note that the error bars are only shown for $\gamma = 0.8$ for clarity purpose.

When $\gamma = 0.8$, the simulated restoration curve fits the real curve the best, which indicates that in practice the rules of restoration sequences are not strictly obeyed, but are followed for the most part. Also, in the simulation, the economic loss consisting of damaged component repair cost and customer power interruption cost is computed. The average economic loss for $\gamma = 0.8$ is \$530.941 million, which is close to the estimation by Quanta Technology for CenterPoint Energy under Hurricane Ike (\$700.00 million for the whole 2.26 million customers, and as an approximation it is \$526.549 million for the 1.70 million customers in Harris County as the focus area for this study) [34]. However, if $\gamma = 0$ and $\gamma \to \infty$, the average economic losses are \$576.523 million and \$488.558 million, respectively, which indicates the importance of restoration sequences. Compared to the real restoration process, the strict restoration sequences can save up to \$42.383 million, while the random restoration will lead to an additional loss of \$45.582 million.

4. Hurricane resilience assessment

During the restoration process, damaged components are repaired and the system performance can be measured by different metrics, such as the percentage of energized transmission substations (including the non-damaged and repaired ones, which also applies to the following three metrics), the percentage of distribution nodes with power, the percentage of critical facilities with power, and the percentage of customers with power. The first two metrics provide input to the technical resilience estimation, the third one relates to the organizational resilience, and the forth one to the social resilience. Also, the economic loss consisting of damaged component repair cost and customer power interruption cost is estimated as an alternative of the input to economic resilience assessment. Different dimensions of resilience support different angles of decision making. To provide comparisons among the different performance metrics, their changes in terms of restoration time are presented in Fig. 6 for Hurricane Ike. Similar to the results in Fig. 5, the minimum/maximum error bars for each curve are very small, so they are not shown for clarity.

From the figure, it can be seen that the critical facilities and the transmission substations are repaired very quickly. After four to five days, almost all the critical facilities and transmission substations are back to work. Particularly, after 8 h in the aftermath of the

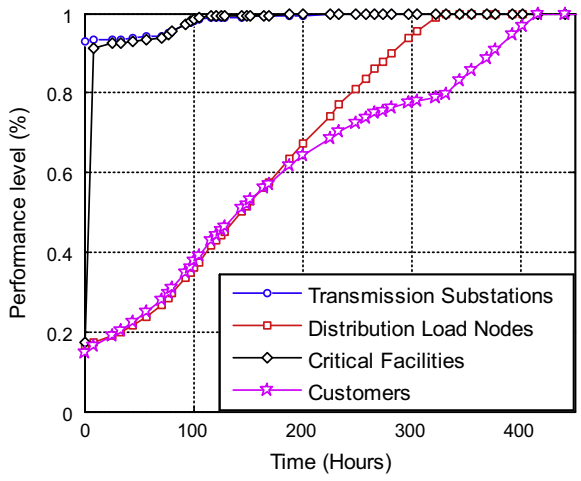

Fig. 6. Restoration curves when the performance levels are measured by different metrics. Points at a specific time in the figure represent the percentage of non-damaged and repaired transmission substations, the percentage of non-damaged and repaired distribution nodes, the percentage of critical facilities with power restored or without power outage, and the percentage of customers with power restored or without power outage.

hurricane, 90% of critical facilities have power supply. These results are consistent with the post-Hurricane-Ike restoration reports [46]. The transmission network is robust under the Hurricane Ike, as only 8% of the substations suffered damage or disconnections from the power plants. However, for the distribution nodes, 85% of them are damaged or disconnected from the power plants. The customers are closely associated with the distribution nodes, so in the initial stage of restoration, the two curves almost overlap until the time 200 h. After that, some crews start repairing the local distribution circuits to later restore power to individual customers, around time 330 h when all distribution nodes have been repaired, and after which the crews can focus on the repair of local distribution circuits and customer tapping points where the curve increases almost linearly.

Next, simulating the hurricane hazards during a time period according to the procedures introduced in Section 2.2, the different dimensions of resilience can then be computed based on Eq. (1). For different hurricane categories, different amounts of resources may be required to reach adequate restoration times. According to the CenterPoint Energy's restoration objectives [46], the expected restoration time for each hurricane category 1–5 should be 7–10 days, 2–3 weeks, 3–5 weeks, 4–6 weeks, and 6–8 weeks, respectively, with some individual customers left for an extended time. Using the same restoration mobilization process after Hurricane Ike for other hurricane categories, it is found that the average restoration times for hurricane categories 1–5 are respectively 8.9 days, 2.3 weeks (2.6 weeks for the Hurricane Ike case), 3.4 weeks, 4.9 weeks and 6.7 weeks, which indicates the proposed model could realistically simulate and approximate the restoration process under different hurricane categories. Then, set the time period $T = 100$ years to capture hurricanes with categories 4–5, and run the simulation 10,000 times (note that for the *current potential resilience* considered in this paper, according to Eq. (2), the value of T does not affect the expected resilience, it only affects its uncertainty or probability distribution). Then, the technical resilience for transmission substations R_{TT}, the technical resilience for distribution nodes R_{TD}, the organizational resilience for critical facilities R_{OC}, and the social resilience for customers R_{SC}, respectively, have an expected value of $R_{TT}(100) = 99.962\%$, $R_{TD}(100) = 99.791\%$, $R_{OZ}(100) = 99.964\%$, $R_{SC}(100) = 99.760\%$. The complementary cumulative distribution function for the 10,000 resilience values in each case is presented in Fig. 7 to capture the resilience distribution. To clearly show these curves in the same plot, the resilience $R(100)$ is shown in a logarithmic form $-\log_{10}(1 - R(100))$. This logarithmic expression is intended to facilitate resilience comparisons and resilience communication, in the same spirit as the classical reliability index did for comparing small failure probabilities in practice.

From the figure, the organizational resilience is the highest, followed by the technical resilience at the transmission level. Their average resilience values are very close because they are strongly correlated. According to the rules of the restoration sequences, the transmission substations and the critical facilities have the same priority, which means that once a damaged or disconnected substation serving some critical facilities has been repaired, then those critical facilities can immediately get back to work. However, there also exist the probability that all critical facilities are repaired, while there are still some remaining damaged substations not serving any critical facility, so the average value of $R_{OZ}(100)$ is slightly higher than that of $R_{TT}(100)$. Similarly, the social resilience and the technical resilience at the distribution level are also correlated because a distributed node must be repaired before the power recovery of its served customers. Hence, the average value of $R_{SC}(100)$ is smaller than that of $R_{TD}(100)$. Also, the economic loss, as an alternative metric of economic resilience, is on average \$82.654 million per year among all simulation runs.

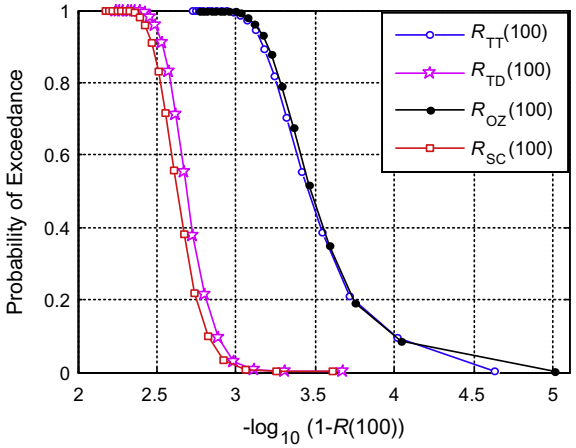

Fig. 7. Probabilistic description of different dimensions of resilience $R(100)$. The performance levels are respectively measured by the percentage of transmission substations with power, the percentage of distribution nodes with power, the percentage of critical facilities with power, and the percentage of customers with power, corresponding to technical resilience on transmission system R_{TT}, technical resilience on distribution system R_{TD}, organizational resilience R_{OZ}, and social resilience R_{SC}, respectively. The resilience $R(100)$ is shown in a logarithmic form $-\log_{10}(1 - R(100))$, where $-\log_{10}(1 - R(100)) = 2$ means $R(100) = 0.99$, $-\log_{10}(1 - R(100)) = 3$ means $R(100) = 0.999$, $-\log_{10}(1 - R(100)) = 4$ means $R(100) = 0.9999$ ad infinitum.

Furthermore, the resilience model introduced in Section 2 has many input parameters, but the resilience $R(100)$ has similar probabilistic distribution curves for repetitions of the 10,000 simulations several times, and the range of $R(100)$ in the logarithmic spaces, as shown in the horizontal axis of Fig. 7, has a narrow distribution, which indicates controlled uncertainty for the resilience under a time interval $T = 100$ years mainly because more hurricane events in general take place and the statistical analyses are more robust to larger samples. However, many of the system and model input parameters can be enhanced for resilience improvement and economic loss reduction. Hence, this paper considers next the effects of some typical parameter variations that can trigger system-level resilience improvements. These parameters can be effectively improved in practice or are considered as main improvement strategies by utility companies, including the change of the restoration sequence control factor γ, the adjustment of resource mobilization curves I_R, and the enhancement of the rate of under-grounding distribution lines f_u. The specific adjustment parameters and the corresponding resilience changes as well as the average economic loss are listed in Table 1.

From the table, when the different strategies are implemented, the average technical resilience R_{TT} and the average organizational resilience R_{OC} remain almost constant, while the average values of the other two resilience dimensions vary largely. If the restoration sequence control factor γ increases from 0 to 0.8 and from 0.8 to ∞, the improvement magnitudes of the average value of R_{TD} (or R_{SC}) in logarithmic spaces are 0.02 (0.06) and 0.015 (0.053), respectively, while the average annual economic savings are \$4.596 million (from 0 to 0.8) and \$5.331million (from 0.8 to ∞). If the hourly resource increase I_R increases from 0 to 15 and from 15 to 30, the improvement magnitudes of the average value of R_{TD} (or R_{SC}) in logarithmic spaces are 0.317 (0.326) and 0.117 (0.129), respectively, and the annual economic savings are \$38.72 million and \$8.761 million. Finally, if the under-grounding rate f_u increases from 0.32 to 0.50, the improvement magnitude of average value of R_{TD} (or R_{SC}) in the logarithmic space is 0.121 (0.107), with economic savings of \$14.774 million. These results show that a small improvement on resilience can save millions of economic loss per year because of the aggregation of the distributed effects

Table 1
Resilience variation under different improvement strategies.

Strategy	Average resilience (logarithmic value)		Average economic loss (millions of U.S. dollars per year)
Original	R_{TT}	99.962% (3.426)	$82.654
	R_{TD}	99.791% (2.681)	
	R_{OC}	99.964% (3.445)	
	R_{SC}	99.760% (2.620)	
$\gamma = 0$	R_{TT}	99.962% (3.426)	$87.985
	R_{TD}	99.782% (2.661)	
	R_{OC}	99.964% (3.444)	
	R_{SC}	99.724% (2.560)	
$\gamma \to \infty$	R_{TT}	99.961% (3.408)	$78.058
	R_{TD}	99.799% (2.696)	
	R_{OC}	99.964% (3.443)	
	R_{SC}	99.788% (2.673)	
$I_R = 0$	R_{TT}	99.960% (3.398)	$121.374
	R_{TD}	99.567% (2.364)	
	R_{OC}	99.961% (3.407)	
	R_{SC}	99.492% (2.294)	
$I_R = 30$	R_{TT}	99.963% (3.433)	$73.893
	R_{TD}	99.841% (2.798)	
	R_{OC}	99.964% (3.446)	
	R_{SC}	99.822% (2.749)	
$f_u = 0.5$	R_{TT}	99.964% (3.439)	$67.880
	R_{TD}	99.842% (2.802)	
	R_{OC}	99.965% (3.452)	
	R_{SC}	99.813% (2.727)	

across the system. However, to choose an optimum improvement strategy, additional analysis would be required to quantify the cost of these strategies, so that a full optimum multi-constrain cost-benefit analysis can help identifying the best improvement strategy or combination of strategies. This analysis is outside the scope of this paper due to data paucity. In the future, the authors will summarize a series of resilience improvement strategies, including smart grid techniques, as well as their costs, and integrate other hazard types to provide a comprehensive cost-benefit analysis to find out the optimum retrofit strategy within a lifecycle context.

5. Conclusions

Electric grid resilience is the joint ability of power systems to resist plausible hazards, absorb the initial damage, and rapidly restore to normal operation. This definition requires the resilience assessment to account for relevant hazards, system cascading failures, and restoration processes. Each of these aspects needs different models and abundant data to approach reality. To capture the essential factors affecting hurricane resilience assessment of critical power systems, this work builds upon available literature and studies of the emergency operation plans of utility companies for hurricane events, to then introduce a probabilistic model to assess the multi-dimensional hurricane resilience of electric power systems. This approach enhances the information provided by traditional reliability assessments and available resilience studies. The probabilistic resilience model includes a Poisson process model of hurricane occurrence during a time period, fragility models for multiple components, a DC power flow model for power system performance, and a power system restoration model with the consideration of component repair priority. Also, as the need for resilience communication increases, this paper presents the typically high absolute value of resilience in a logarithmic scale to emulate what the reliability index did in the reliability design community. Also, based on real customer outage and restoration data of the electric power system in Harris County, Texas in the aftermath of Hurricane Ike in 2008, the resilience model is calibrated to show the outputs' consistency with real data, to then assess and compare different resilience improvement strategies. Results show that among the technical, organizational and social dimensions, the organizational resilience is the highest with a value of 3.445 in the logarithmic scale while the social resilience is the lowest with a value of 2.620 in the same scale. To improve system resilience and reduce economic loss, strictly obeying the restoration sequences, increasing the restoration resources and their mobilization rate, and enhancing the rate of under-grounding critical distribution lines are all effective strategies in practice.

Note that this paper defines resilience unconditionally by accounting for a multiplicity of hazard levels and their probability of occurrence, which leads to high resilience values. The authors also recognize, as shown for hurricane Ike, that scenario-based contingency analyses are also part of the best engineering practices, and the system should be checked for likely and unlikely scenarios and determine how well they perform; however, this type of system assessment under specific events is better referred to as "vulnerability" analysis, which is aimed at specific events and can be quantified as the system consequences (which may also include the restoration effects) under the event [4]. The proposed unconditional resilience can complement traditional scenario-based approaches for the ultimate goal of informing design guidelines that are based on resilience and multiple hazards [50,51]. Also, the resilience metric in this paper is related to power industry standard reliability measures, such as SAIFI (System Average Interruption Frequency Index) and SAIDI (System Average Interruption Duration Index), which are usually computed by classical reliability assessment methods but typically excluding major event days [52]. These reliability assessment methods usually model the restoration time through random variables with distribution parameters estimated from historical data, whereas the resilience assessment requires modeling the hazards, emergency responses and restoration efforts in more detail to analyze and compare the robustness and rapidity improvements under different response techniques and strategies.

However, the proposed hurricane resilience model is still a streamlined version of the real power grid response seen in practice and provides an initial framework and an initial step to quantify power system resilience to support resilience-based decisions and design for distributed lifeline systems. Applying the model to other power systems, as utility companies may have different emergency operation plans, mutual assistance programs and component restoration priorities, requires adapting the restoration model besides changing some system parameter values, such as hazard type and return periods, component fragility curves for the specific hazard type, power injection data, line impedance, amount of resources and their mobilization rate, among others. Also, when more data are available, some component fragility models, such as the wind-throw-induced distribution line fragility, and the modeling of distribution networks and local distribution circuits should be improved, along with comparisons of different resilience improvement strategies, including emerging smart grid techniques. In addition, power systems are interdependent with other utility systems [1,31] and need explicit consideration. Hurricane events can hit many of these systems simultaneously, so integrating interdependencies into resilience analysis along with emerging frameworks for performance-based goals [54], constitutes a promising avenue for resilience assessment enhancement.

Acknowledgments

This work was supported in part by the U.S. National Science Foundation under Grant CMMI-0748231, the National Science Foundation of China under Grant 51208223, and the Independent Innovation Foundation of Huazhong University of Science and Technology under Grant 2012QN088. Any opinions, findings, and

conclusions or recommendations expressed in this material are those of the authors and do not necessarily reflect the views of the sponsors. The authors also wish to thank Rice University and the Office of Public Safety and Homeland Security of the City of Houston for their support.

References

[1] Ouyang M. Review on modeling and simulation of interdependent critical infrastructure systems. Reliab Eng Syst Safe 2014;121:43–60.
[2] National Hurricane Center; 2010. http://www.nhc.noaa.gov/pastprofile.shtml.
[3] Haimes YY. On the definition of resilience in systems. Risk Anal 2009;29(4):498–501.
[4] Aven T. On some recent definitions and analysis frameworks for risk, vulnerability and resilience. Risk Anal 2011;31:515–22.
[5] Kahan JH, Allen AC, George JK. An operational framework for resilience. J Homeland Secur Emergency Manage 2009;6(1). article 83.
[6] Mili L. Taxonomy of the characteristics of the power system states. In: Proceedings of the second NSF-RESIN workshop on resilient and sustainable critical infrastructures, January 13–15, 2011, Tuscon, AZ; 2011. http://www.nvc.vt.edu/lmili/publications.html.
[7] Plodinec MJ. Definitions of resilience: an analysis. Community and Regional Resilience Institute; 2009. p. 1–17. http://www.resilientus.org/library/CARRI_Definitions_Dec_2009_1262802355.pdf.
[8] Ouyang M, Duenas-Osorio L. A three-stage resilience analysis framework for urban infrastructure systems. Struct Saf 2012;36:23–31.
[9] Bruneau M, Chang SE, Eguchi RT, Lee GC, O'Rourke TD, Reinhorn AM, et al. A framework to quantitatively assess and enhance the seismic resilience of communities. Earthquake Spectra 2003;19(4):733–52.
[10] Bruneau M, Reinhorn AM. Exploring the concept of seismic resilience for acute care facilities. Earthquake Spectra 2007;23(1):41–62.
[11] Cimellaro G, Reinhorn A, Bruneau M. Framework for analytical quantification of disaster resilience. Eng Struct 2010;32:3639–49.
[12] Chang SE, Shinozuka M. Measuring improvements in the disaster resilience of communities. Earthquake Spectra 2004;20(3):739–55.
[13] Reed DA, Kapur KC, Christie RD. Methodology for assessing the resilience of networked infrastructure. IEEE Syst J 2009;3(2):174–80.
[14] Vugrin ED, Warren DE, Ehlen MA, Camphouse RC. A framework for assessing the resilience of infrastructure and economic systems. In: Kasthurirangan Gopalakrishnan, Peeta Srinivas, editors. Sustainable and resilient critical infrastructure systems: simulation, modeling, and intelligent engineering. Springer-Verlag, Inc.; 2010.
[15] O'Rourke TD. Critical infrastructure, interdependencies, and resilience. The Bridge-Linking Engineering and Society; Spring 2007. p. 22–29. http://www.nae.edu/Publications/Bridge/EngineeringfortheThreatofNaturalDisasters/CriticalInfrastructureInterdependenciesandResilience.aspx.
[16] Zobel CW. Representing perceived tradeoffs in defining disaster resilience. Decis Support Syst 2010;50:394–403.
[17] Ouyang M, Dueñas-Osorio L. Time-dependent resilience assessment and improvement of urban infrastructure systems. Chaos 2012;22(3):033122-1–033122-11.
[18] Poljansek K, Bono F, Gutierrez E. Seismic risk assessment of interdependent critical infrastructure systems: the case of European gas and electricity networks. Earthquake Eng Struct Dynam 2012;41:61–79.
[19] Duenas-Osorio L, Craig JI, Goodno BJ. Seismic response of critical interdependent networks. Earthquake Eng Struct Dynam 2007;36:285–306.
[20] Adachi T, Ellingwood BR. Serviceability of earthquake-damaged water systems: effects of electrical power availability and power backup systems on system vulnerability. Reliab Eng Syst Saf 2008;93:78–88.
[21] Patterson SA, Apostolakis GE. Identification of critical locations across multiple infrastructures for terrorist actions. J Reliab Eng Syst Saf 2007;92(9):1183–203.
[22] Duenas-Osorio L, Vemuru SM. Cascading failures in complex infrastructure systems. Struct Saf 2009;31(2):157–67.
[23] Cagnan Z, Davidson RA, Guikema SD. Post-earthquake restoration planning for Los Angeles electric power. Earthquake Spectra 2006;22(3):589–608.
[24] Xu NX, Guikema SD, Davidson RA, Nozick LK, Cagnan Z, Vaziri K. Optimizing scheduling of post-earthquake electric power restoration tasks. Earthquake Eng Struct Dynam 2007;36:265–84.
[25] Anghel M, Werley KA, Motter AE. Stochastic model for power grid dynamics. In: Fortieth Hawaii international conference on system sciences, January 3–6, 2007, Big Island, Hawaii; 2007.
[26] Platts. Topology of the State of Texas power transmission network; 2009. http://www.platts.com/ [accessed 05/2009].
[27] Bayliss C, Hardy B. Transmission and distribution electrical engineering. 3rd ed. Elsevier Ltd; 2007.
[28] Short TA. Electric power distribution handbook. Boca Raton: CRC Press; 2004.
[29] Winkler J, Dueñas-Osorio L, Stein R, Subramanian D. Performance assessment of topologically diverse power systems subjected to hurricane events. Reliab Eng Syst Saf 2010;95(4):323–36.
[30] Quanta Technology. Undergrounding assessment phase 3 final report: ex ante cost and benefit modeling. Prepared for the Florida Electric Utilities and submitted to the Florida Public Service Commission per order PSC-06-0351-PAA-EI; May 2008.
[31] Ouyang M, Dueñas-Osorio L. An approach to design interface topologies across interdependent urban infrastructure systems. Reliab Eng Syst Saf 2011;96(11):1462–73.
[32] Federal Emergency Management Agency. Hazards U.S. Multi-Hazard (HAZUS-MH) Assessment Tool v1.3; 2011. www.fema.gov/plan/prevent/hazus/index.shtm.
[33] Wong CJ, Miller MD. Guidelines for electrical transmission line structure loading. ASCE manuals and reports on engineering practice No. 74; 2010.
[34] Quanta Technology. Cost benefit analysis of the deployment utility infrastructure upgrades and storm hardening programs. Technical Report No. 36375 for the Public Utility Commission of Texas; 2009.
[35] Fenton GA, Sutherland N. Reliability-based transmission line design. IEEE Trans Power Del 2011;26(2):596–606.
[36] Dagher HJ. Reliability-based design of utility pole structures. ASCE manuals and reports on engineering practice No. 111; 2006.
[37] Canham CD, Papaik MJ, Latty EF. Interspecific variation in susceptibility to wind-throw as a function of tree size and storm severity for northern temperate tree species. Can J For Res 2001;31(1):1–10.
[38] Vickery PJ, Lin J, Skerlj PF, Twisdale LA, Huang K. HAZUS-MH hurricane model methodology. I: hurricane hazard, terrain, and wind load modeling. Nat Hazards Rev 2006;7:82–90.
[39] LaCommare KH, Eto JH. Cost of power interruptions to electricity consumers in the United States (US). Energy 2006;31(12):1845–55.
[40] Dobson I, Carreras BA, Lynch VE, Newman DE. Complex systems analysis of series of blackouts: cascading failure, critical points and self-organization. Chaos 2007;17(2):026103.
[41] Kirschen DS, Jayaweera D, Nedic DP, Allan RN. A probabilistic indicator of system stress. IEEE Trans Power Syst 2004;19:1650–7.
[42] Chen J, Thorp JS, Dobson I. Cascading dynamics and mitigation assessment in power system disturbance via a hidden failure model. Electr Power Energy Syst 2005;27:318–26.
[43] Nateghi R, Guikema SD, Quiring SM. Comparison and validation of statistical methods for predicting power outage durations in the event of hurricanes. Risk Anal 2011;31(12):1897–906.
[44] Liu HB, Davidson RA, Apanasovich T. Statistical forecasting of electric power restoration times in hurricanes and ice storms. IEEE Trans Power Syst 2007;22(4):2270–9.
[45] Liu H. Statistical modeling of electric power outage counts and restoration times during hurricanes and ice storms [Ph.D. thesis]. Cornell University; 2006.
[46] Centerpoint Energy. Centerpoint energy Ike storm center. www.centerpointenergy.com/newsroom/stormcenter/ike.
[47] Miller LM, Antonio RJ, Bonanno A. Hazards of neoliberalism: delayed electric power restoration after Hurricane Ike. Br J Sociol 2011;62(3):504–22.
[48] Ouyang M. Comparisons of Purely topological model, betweenness based model and direct current power flow model to analyze power grid vulnerability. Chaos 2013;23:023114.
[49] The hurricane research group at Rice University conducted a "Hurricane Ike survey" (led by Professor Robert M. Stein and research scientist Birnur Buzcu-Guven), with 1498 residents in Harris County in the aftermath of Hurricane Ike. The survey data, which includes demographic and other hurricane evacuation data is available from Prof. Stein (email: stein@rice.edu), and show the number of customers who are subject to a combination of a level of power outage (extremely serious, very serious, somewhat serious, not serious, did not happen) and an extent of tree wind-throw (extremely serious, very serious, somewhat serious, not serious, did not happen) nearby their houses. The power outage levels are mainly judged according to their experienced outage length. Those customers who experienced serious power outages provide indirect evidence that the local distribution circuits nearby their houses were also damaged because according to restoration sequences, the local distribution circuits have the last repair priority, and only the customers who have their local circuits damaged could experience significantly long outages. Hence, computing the total cases of tree wind-throw (including somewhat serious, very serious, and extremely) (972 cases), and the total cases of extremely serious power outage in the case of tree wind-throw (506 cases) can provide an estimated probability of 0.52 of a customer losing power due to damage on local distribution circuits in case of tree wind-throw, which is just the parameter β.
[50] Sunder SS. NIST (National Institute of Standards and Technology) disaster resilience programs overview. In: ACEHR meeting, November 8, 2011. http://www.nehrp.gov/pdf/ACEHRNov2011_Sunder.pdf.
[51] ASCE (American Society of Civil Engineers). Guiding principles for the nation's critical infrastructure, prepared by the ASCE Critical Infrastructure Guidance Task Committee; 2009. http://content.asce.org/files/pdf/GuidingPrinciplesFinalReport.pdf.
[52] Eto JH, LaCommare KH. Tracking the reliability of the U.S. electric power system: an assessment of publicly available information reported to state public utility commissions. http://certs.lbl.gov/pdf/lbnl1092e-puc-reliability-data.pdf.
[53] Texas Electricity Alliance. http://texaselectricityalliance.wordpress.com/.
[54] Barbato M, Petrini F, Unnikrishnan VU, Ciampoli M. Performance-Based Hurricane Engineering (PBHE) framework. Struc Saf 2013;45:24–35. http://dx.doi.org/10.1016/j.strusafe.2013.07.002.